



Regulation of hepatic cardiolipin metabolism by $\text{TNF}\alpha$: Implication in cancer cachexia

Laure Peyta, Kathleen Jarnouen, Michelle Pinault, Cédric Coulouarn, Cyrille Guimaraes, Caroline Goupille, Jean-Paul Pais de Barros, Stephan Chevalier, Jean-François Dumas, François Maillot, et al.

► To cite this version:

Laure Peyta, Kathleen Jarnouen, Michelle Pinault, Cédric Coulouarn, Cyrille Guimaraes, et al.. Regulation of hepatic cardiolipin metabolism by $\text{TNF}\alpha$: Implication in cancer cachexia. BBA - Biochimica et Biophysica Acta, 2015, 1851 (11), pp.1490-1500. 10.1016/j.bbali.2015.08.008 . hal-01197346

HAL Id: hal-01197346

<https://hal-univ-rennes1.archives-ouvertes.fr/hal-01197346>

Submitted on 21 Sep 2015

HAL is a multi-disciplinary open access archive for the deposit and dissemination of scientific research documents, whether they are published or not. The documents may come from teaching and research institutions in France or abroad, or from public or private research centers.

L'archive ouverte pluridisciplinaire **HAL**, est destinée au dépôt et à la diffusion de documents scientifiques de niveau recherche, publiés ou non, émanant des établissements d'enseignement et de recherche français ou étrangers, des laboratoires publics ou privés.

Regulation of hepatic cardiolipin metabolism by TNF α : implication in cancer cachexia

Laure Peyta¹, Kathleen Jarnouen^{2,3}, Michelle Pinault¹, Cedric Coulouarn^{2,3}, Cyrille Guimaraes¹, Caroline Goupille^{1,5}, Jean-Paul Pais de Barros⁴, Stephan Chevalier¹, Jean-François Dumas¹, François Maillot^{1,5}, Grant M. Hatch⁶, Pascal Loyer^{2,3} and Stephane Servais¹.

¹Inserm UMR1069, *Nutrition, Croissance et Cancer*, Université François Rabelais de Tours- 10, bd Tonnellé - 37032 Tours Cedex, France. laure.peyta@etu.univ-tours.fr; michelle.pinault@univ-tours.fr; cyrille.guimaraes@gmail.com; caroline.goupille@univ-tours.fr; stephan.chevalier@univ-tours.fr; jean-francois.dumas@univ-tours.fr; maillot@med.univ-tours.fr; stephane.servais@univ-tours.fr

²Inserm UMR S-991, *Foie, Métabolismes et Cancer*, CHU Pontchaillou, 2 rue Henri Le Guilloux, 35033 Rennes, France. kathleen.jarnouen@univ-rennes1.fr; cedric.coulouarn@univ-rennes1.fr; pascal.loyer@univ-rennes1.fr

³Université de Rennes 1, 2 rue du Thabor CS46510, 35065 Rennes cedex, France.

⁴Plateforme de Lipidomique. INSERM UMR866 / LabEx LipSTIC, 15 Bd Mal de Lattre de Tassigny, 21000 Dijon, France. jppais@u-bourgogne.fr

⁵CHRU de Tours, Département de Médecine Interne, 2, boulevard Tonnellé - 37044 Tours cedex 9, France.

⁶Department of Pharmacology and Therapeutics, Biochemistry and Medical Genetics, Faculty of Health Sciences, Center for Research and Treatment of Atherosclerosis, DREAM Children's Hospital Research Institute of Manitoba, University of Manitoba, 513 – 715 McDermot Avenue Winnipeg MB R3E 3P4, Manitoba, Canada. ghatch@chrim.ca

*Corresponding author:

Stephane SERVAIS, Laboratoire Nutrition, Croissance et Cancer - Inserm UMR1069

Faculté de Médecine - 10, bd Tonnellé - 37032 Tours Cedex

Email stephane.servais@univ-tours.fr; Phone +33 2.47.36.60.59; Fax +33 2 47 36 62 26

Running title: cardiolipin metabolism in cancer cachexia

Abbreviations: ALCAT1: acyl-CoA:lysocardiolipin acyltransferase; CDP-DAG: diphosphate-1,2-diacyl-sn-glycerol; CDS:cytidine-5'-diphosphate-1,2-diacyl-sn-glycerol synthase; CL: cardiolipin; CLS: cardiolipin synthase; DMSO: dimethylsulfoxide; ETS: electron transfert system; FCCP: Carbonyl cyanide-4-(trifluoromethoxy)phenylhydrazone; GAPDH: glyceraldehyde 3-phosphate dehydrogenase; Hsc70: Heat shock cognate 70 kDa; iPLA2 γ :calcium independent phospholipase A2 gamma; MLCL AT-1: monolysocardiolipin acyltransferase-1; MLCL: monolysocardiolipin; PC: phosphatidylcholine; PCC: peritoneal carcinosis induced cachexia; PE: phosphatidylethanolamine; PF: pair fed; PG: phosphatidylglycerol; PGC-1 α : peroxisome proliferator-activated receptor gamma coactivator 1-alpha; PGP: phosphatidylglycerol phosphate; PGPP: phosphatidylglycerol phosphate phosphatase; PGPS: phosphatidylglycerol phosphate synthase; PI: phosphatidylinositol; PS: phosphatidylserine; SM: sphingomyelin; TAZ: tafazzin; TNF α : tumor necrosis factor alpha; VDAC: voltage-dependent anion channel.

Abstract

Cardiolipin (CL) content accumulation leads to an increase in energy wasting in liver mitochondria in a rat model of cancer cachexia in which tumor necrosis factor alpha (TNF α) is highly expressed. In this study we investigated the mechanisms involved in liver mitochondria CL accumulation in cancer cachexia and examined if TNF α was involved in this process leading to mitochondrial bioenergetics alterations. We studied gene, protein expression and activity of the main enzymes involved in CL metabolism in liver mitochondria from a rat model of cancer cachexia and in HepaRG hepatocyte-like cells exposed to 20 ng/ml of TNF α for 12 h. Phosphatidylglycerolphosphate synthase (PGPS) gene expression was increased 2.3-fold ($p<0.02$) and cardiolipin synthase (CLS) activity decreased 44% ($p<0.03$) in cachectic rat livers compared to controls. CL remodeling enzymes monolysocardiolipin acyltransferase (MLCL AT-1) activity and tafazzin (TAZ) gene expression were increased 30% ($p<0.01$) and 50% ($p<0.02$), respectively, in cachectic rat livers compared to controls. Incubation of hepatocytes with TNF α increased CL content 15% ($p<0.05$), mitochondrial oxygen consumption 33% ($p<0.05$), PGPS gene expression 44% ($p<0.05$) and MLCL AT-1 activity 20% ($p<0.05$) compared to controls. These above findings strongly suggest that in cancer cachexia, TNF α induces a higher energy wasting in liver mitochondria by increasing CL content *via* upregulation of PGPS expression.

Highlights:

- First demonstration of liver cardiolipin metabolism alteration in cancer induced cachexia
- Direct implication of TNF α in mitochondrial energy wasting via cardiolipin modulation
- Increasing knowledge on cellular mechanism of liver energetic alteration during cancer cachexia

Key words: cardiolipin biosynthesis, cytokines, mitochondria, energy wasting, liver, cardiolipin remodeling, inflammation.

INTRODUCTION

Cancer cachexia is a multifactorial syndrome characterized by a progressive deterioration of nutritional status due to whole body negative energy balance driven by a reduced calorie intake (anorexia) and/or inappropriate energy expenditure (hypermetabolism) and systemic inflammation [1]. Depending on tumor type, cancer cachexia occurs in 30 to 80% of patients [2–4]. The negative energy balance induces white adipose tissue and skeletal muscle wasting which both impair quality of life and increase chemo- and radiotherapy associated toxicity in patients [5]. The mechanisms of cancer cachexia have not been fully elucidated and this explains the difficulties in managing therapy and restoring nutritional status in cancer patients. We recently investigated mechanisms involved in the hypermetabolism observed during cachexia in a rat preclinical model peritoneal carcinosis [6]. We demonstrated that peritoneal carcinosis-induced cachexia was associated with bioenergetic alterations in the healthy liver. Liver mitochondria from cachectic rats displayed significant increases in energy wasting and this was associated with reduced ATP production yield. Interestingly, liver mitochondria cardiolipin (CL) content was increased in cachectic rats in comparison to healthy controls [7]. Importantly, CL content was positively correlated with this increase in energy wasting. We subsequently demonstrated *in vitro* that CL content was indeed directly involved in the increase in liver mitochondria energy wasting [8]. Cancer cachexia not only affected the CL content but also CL fatty acid composition in liver mitochondria [6]. The mechanisms driving such liver mitochondrial CL alterations in cancer cachexia have not been investigated.

CL [bis-(1,2-diacyl-*sn*-glycero-3-phospho)-1'-3'-*sn*-glycerol] is a major and specific phospholipid of the mitochondria and on the inner membrane CL is required for the activity of a number of key mitochondrial enzymes involved in cellular energy metabolism [9,10]. CL metabolism is complex and includes both *de novo* biosynthesis and remodeling. In mammals, the first step of CL *de novo* synthesis is catalyzed by cytidine-5'-diphosphate-1,2-diacyl-*sn*-glycerol synthase (CDS) producing diphosphate-1,2-diacyl-*sn*-glycerol (CDP-DAG). Phosphatidylglycerol phosphate synthase (PGPS), the committed step of CL synthesis, catalyzes the formation of phosphatidylglycerol phosphate (PGP) from CDP-DAG. PGP is then dephosphorylated to phosphatidylglycerol (PG) by PGP phosphatase (PGPP) [11]. The final step is catalyzed by CL synthase (CLS) [12]. At this step CL is considered as nascent and will undergo

maturation by fatty acyl remodeling. Remodeling allows the formation of mature CL with defined fatty acyl composition. Initially deacylation by calcium independent phospholipase A₂ (iPLA₂ γ) as well as other putative phospholipases [13] produces monolysocardiolipin (MLCL), this step is followed by resynthesis catalyzed by at least 3 enzymes: monolysocardiolipin acyltransferase-1 (MLCL AT-1), acyl-CoA:lysocardiolipin acyltransferase (ALCAT1) or the transacylase tafazzin (TAZ) [14–16].

Whereas there is a relative consensus about CL *de novo* synthesis in yeast and lower eukaryotes, regulation of the CL metabolic enzymes in higher eukaryotes is still poorly understood [17]. Previous studies in heart and myoblasts indicated that CL metabolism was upregulated by peroxisome proliferator-activated receptor α agonist [18] and peroxisome proliferator-activated receptor gamma coactivator 1-alpha (PGC-1 α) [19]. Since inflammation is a hallmark of cancer cachexia [20], we hypothesized that inflammatory cytokines may play a significant role in the dysregulation of CL metabolism in cancer cachexia and energy wasting increase in liver mitochondria. Our previous study clearly highlighted TNF α as the major cytokine (14-fold elevated serum concentration) in our preclinical model of cancer cachexia [6].

The aim of the present study was to investigate the mechanisms responsible for liver mitochondrial CL accumulation and its altered fatty acid composition in cancer cachexia. We examined gene expression, protein expression and activity of the main enzymes involved in CL biosynthesis and remodeling in liver mitochondria from a preclinical model of cancer cachexia [6]. In addition, we investigated the *in vitro* effect of the proinflammatory cytokine TNF α on CL metabolism related enzymes in the human hepatoma HepaRG hepatocyte-like cells that retain many characteristics of primary human hepatocytes [21].

MATERIALS AND METHODS

Materials

Undifferentiated HepaRG cells (BioPredict International France, Batch number HPR101007-A), [^{14}C]Glycerol-3-phosphate, [$5\text{-}^3\text{H}$]Cytidine 5'-riphosphate, [$1\text{-}^{14}\text{C}$]palmitoyl-phosphatidylcholine, [$1\text{-}^{14}\text{C}$]linoleoyl-Coenzyme A were obtained from Dupont, Mississauga, Ontario, Canada or Amersham, Oakville, Ontario, Canada. [^{14}C]PG was synthesized from [^{14}C]glycerol-3-phosphate as described [22].

Animal model

Liver from cachectic (peritoneal carcinosis induced cachexia, PCC) and healthy (pair fed, PF) rats were obtained as previously described [6].

Cell culture and treatments for in vitro inflammation study

As previously described [21] HepaRG cells line were cultivated in William's E medium supplemented with 10% fetal bovine serum, 100 U/ml penicillin, 100 $\mu\text{g/ml}$ streptomycin, 5 $\mu\text{g/ml}$ insulin, and 50 μM hydrocortisone hemisuccinate. After 2 weeks, the medium was supplemented with 2% dimethyl sulfoxide (DMSO) and the cells were cultured for 2 more weeks. HepaRG hepatocytic cells from DMSO treated cultures were selectively detached using gentle trypsinization and seeded at high density for cytokine treatments. Cells were incubated for 12 h with 20 ng/ml of $\text{TNF}\alpha$.

Generation of SiPGPS HepaRG Cells

The validated siRNA (sc-94116, Santa Cruz Biotechnology) was used for knocking down the expression of PGPS in HepaRG hepatocyte-like cells. The siRNA (s1227, Ambion®) targeting albumin was used as control. Electroporation was performed using the Neon® transfection system (Life Technologies) available at the SynNanoVect core facility (Biogenouest, Rennes, France) as previously described [23]. Briefly, differentiated HepaRG hepatocyte-like cells were detached by trypsin incubation, then, 10^6 cells were electroporated with 40 picomoles of siRNA and the following parameters: one pulse of 1500 volts during 20ms. Cells were immediately seeded at the density of 2.5×10^5 cells/cm 2 and cultured in William's

E medium supplemented with 2% DMSO. Twenty four hours after electroporation, medium was discarded and cells were cultured in William's E medium without fetal calf serum and DMSO for 24h prior stimulation with 20 ng/mL of TNF α for 12h.

Transmission electron microscopy for mitochondrial content determination

HepaRG cells and liver biopsies were fixed by incubation for 24 h in 4% paraformaldehyde, 1% glutaraldehyde in 0.1 M phosphate buffer (pH 7.2). Samples were then washed in phosphate-buffered saline (PBS) and post-fixed by incubation with 2% osmium tetroxide for 1 h. Samples were then fully dehydrated in a graded series of ethanol solutions followed by a propylene oxide bath. Pre-impregnation step was made by a propylene oxide/Epon resin mixture (Sigma) and finally overnight in pure resin for impregnation of the samples. Cells were then embedded in Epon resin (Sigma), which was allowed to polymerize for 48 h at 60°C. Ultra-thin sections (90 nm) of these blocks were obtained with a Leica EM UC7 ultramicrotome (Wetzlar, Germany). Sections were deposited on gold grids and stained with 2% uranyl acetate, 5% lead citrate. Observations were made with a JEOL 1011 transmission electron microscope. Images were analysed using ImageJ software (NIH)

Phospholipid classes quantitation

Mitochondria were extracted from HepaRG cells by differential centrifugation. Then mitochondrial lipids were extracted following the protocol of Bligh and Dyer [24]. In order to quantify mitochondrial phospholipids (cardiolipin [CL], phosphatidylethanolamine [PE], phosphatidylinositol [PI], phosphatidylcholine [PC], phosphatidylserine [PS] and sphingomyelin [SM]), standards and samples were loaded on silica plates using Linomat V sample applicator (CAMAG, Muttenz Switzerland). Solvent consisted of chloroform, acetone, acetic acid methanol and water (6/8/2/2/1 v/v/v/v/v) modified from [25]. After migration, the plates were immersed into the following solution (10% wt/vol) copper sulfate in 8% (vol/vol) phosphoric acid solution) and then heated at 160°C for 15 min to stain all of the phospholipids. Quantification was performed using Thin Layer Chromatography-visualizer Reprostar 3[®] and WinCats

VideoScan[®] software (CAMAG, Muttenz Switzerland). Results were expressed in percent of total mitochondrial phospholipids.

CL fatty acid molecular species Analysis by LC-MS²

Lipids were extracted from cell pellets (6-8 millions) according to the method of Folch *et al.* [26].

In brief, cells were spiked with (14:0)4-CL used as internal standard (250 ng, Avanti Polar Lipids, Cogee, Paris, France). Lipids were extracted with 1 mL of saline and 3.5 mL of CHCl₃/MeOH (2/1) for 10 min followed by addition of 1.25 mL CHCl₃ for 10 min and finally 1.25 mL of distilled water for 5 min. Organic phase was collected and dried under vacuum. Lipid extracts were further solubilized in 100 µL of CHCl₃/MeOH/H₂O (60/30/4.5). LCMS/MS analyses were performed with a 1200 series HPLC system coupled to a 6460 triple quadrupole mass spectrometer equipped with a JetStream electrospray ionization source (Agilent Technologies). HPLC separation was achieved with a Zorbax EclipsePlus C18 - 2.1 mm x 100 mm, 1.8 µm column (Agilent Technologies) maintained at 50°C. The mobile phases consisted of ACN, water, 28% NH₃ in water and acetic acid (90/10/0.2/0.5 v/v/v/v) (A) and of IPA, water, 28% NH₃ in water and acetic acid (90/10/0.2/0.5 v/v/v/v) (B). The linear gradient was as follows: 50% B for 5 min, up to 80% B in 10 min, up to 100% in 15 min and maintained at 100 % for 5 min. Column was equilibrated with 50% B for 5 min before each injection. The flow rate was set up at 0.4 mL/min. Four microliters were injected onto the LCMS/MS system. Analyses were performed in negative ion mode by Selected Reaction Monitoring (SRM) as previously described [27].

RNA isolation and real time PCR assay

Total RNA from livers or HepaRG cells were extracted with RNeasy Mini kit (QIAGEN; Cat N° 74106) following manufacturer's instructions. Reverse transcription was performed using 1 µg of total ARN with the High Capacity cDNA Reverse Transcription kit (Applied Biosystems, Part N° 4368813). RNA levels of various genes were determined using Taqman- (HepaRG cells) or SYBR green (rat liver)-based quantitative PCR (qPCR) technology performed using Fast Real-time 7900HT system (Applied Biosystems). The 18S and GAPDH were used as housekeeping genes for rat livers and HepaRG cells, respectively. Data were quantified with the StepOne Plus software v2.2.1 and the results were expressed as relative to pair-fed animals or untreated HepaRG cultures arbitrarily set to 1. Primer sequences: rat 18S

5'-CGGCTACCACATCCAAGGAA -3' and 5'- GCTGGAATTACCGCGGCT-3', rat CDS1 5'- GACTCCAGAACACTGTATCT-3' and 5'- GCTCACAGCAGCAATTTGAT-3', rat PGPS 5'- GGCAGATAAAAATAGCCAAG-3' and 5'- CAATCCACCAGTTCCTGTTCC-3', rat CLS 5'- GAACACTAGCTAAGTACTTC-3' and 5'- ACTGCTGTATTGACCTTGC-3', rat TAZ 5'- CTGAAGTTGATGCGTTGGACC-3' and 5'- TGTACCCAGTCCCCATGGTT-3'. Taqman primers for human GAPDH Hs02758991_g1, human PGPP Hs00864157_g1, human PGPS Hs00375485_m1, human CLS Hs00219512_m1, human MLCL AT-1 Hs00426191_m1, human TAZ Hs00794094_m1, human human ALB (Hs00910225_m1) and human TATA Binding Protein (TBP) (Hs00427620_m1).

Western blotting

Rat liver and HepaRG cell mitochondria were isolated as described [28]. 50 µg of mitochondrial protein were separated on 12% sodium dodecyl sulfate-polyacrylamide gel electrophoresis, transferred onto a polyvinylidene fluoride membrane, and probed with antibodies against CLS (14845-1-AP, Proteintech, Manchester, UK), Heat shock cognate 70 (Hsc70, SC7298, SantaCruz) and Voltage Dependent anion channels (VDAC) (AB14734 Abcam) (loading control) followed by horseradish peroxidase-coupled detection (Pierce ECL Western Blotting Substrate). Secondary antibodies were obtained from SantaCruz. The protein band intensities were analyzed by densitometry (MF-ChemiBIS 3.2, DNR Bioimaging Systems, MultiGauge software, Fujifilm).

Assay of enzyme activities

Rat liver and HepaRG cell mitochondria were isolated as described [28]. CDS, PGPS enzyme activities were determined as described [22]. CL synthase activity was assayed exactly as described by Schlame and Hostetler [29], except that the assay contained 0.05-0.1 mg of protein, the pH of the assay was 8.5 and the samples were sonicated for 10 s in a Branson model 1200 sonicator before incubation. Incubation was at 37°C for 60 min with [14C]PG (sp.radioactivity 45000 d.p.m./nmol). MLCL AT-1 activity was determined as described [30].

High-resolution respirometry

High resolution respirometry was performed using a 2-ml chamber OROBOROS® Oxygraph 2K (Oroboros Instruments, Innsbruck, Austria) at 37°C. Respiration rates were calculated as the time derivative of oxygen concentration measured in the closed respirometer and expressed per million viable cells and corrected by non-mitochondrial oxygen consumption (antimycin A). Intact cells (0.5×10^6 cells per milliliter) were analyzed in their respective energy substrate-containing cultivation medium: ROUTINE respiration (no additions), LEAK respiration (oligomycin-inhibited, 8 $\mu\text{g/mL}$), and ETS (Electron Transfert System) capacity (maximum uncoupled respiration) induced by Carbonyl cyanide-4-(trifluoromethoxy)phenylhydrazone (FCCP, 0.8 mM). Oxygen consumption (O_2) was also measured on permeabilized cells (digitonin 1 $\mu\text{g/mL}$) in respiration buffer (10 mM KH_2PO_4 , 300 mM mannitol, 10 mM KCl, 5 mM MgCl_2 , 1 mM EGTA and 1 mg/ml BSA fatty acid free) at final cell density of 0.5×10^6 cells per milliliter. Pyruvate, malate and succinate were used as respiratory substrates.

Statistical analysis

Data are expressed as means \pm S.E.M. Statistical analyses were performed using GraphPad Prism®. The differences between two groups were evaluated by non parametric Mann Whitney *t*-test. Values showing *p* < 0.05 were considered statistically significant unless otherwise indicated.

RESULTS

Mitochondrial content is unchanged during cancer cachexia

CL is a unique phospholipid only found in mitochondrial membranes. In order to exclude that mitochondrial biogenesis was the origin for CL accumulation (+50%); we first quantified liver mitochondrial mass from PF and PCC rats using electron microscopy. Our results did not show any difference between the two groups of rats (Figure 1). Indeed, hepatocytes from PF rats contained 20.32% \pm 1.95 of mitochondria whereas 22.24% \pm 1.58 for PCC rat hepatocytes.

Liver PGPS and CLS are altered in cancer cachexia

To investigate the biochemical alterations in CL biosynthesis during cancer cachexia four enzymes of CL metabolism were studied: CDS-1, PGPS, PGPP, and CLS in liver of healthy (PF) and cachectic rats (PCC). CDS-1 mRNA level and CDS enzyme activity were similar between PCC and PF rats (Figure 2A and B). In contrast, gene expression of PGPS was significantly increased by 2.3-fold ($p = 0.02$) in liver of PCC compared to PF rats (Figure 2C). In addition, PGPS activity appeared to be increased by 30% in PCC compared to PF rats (Figure 2D) without reaching statistical significance. PGPP mRNA expression was unaltered between PCC and PF rats (0.56 \pm 0.20 and 0.63 \pm 0.14, respectively). CLS mRNA and protein expression were similar between PCC and PF rats (Figure 3 A and B). However, mitochondrial CLS enzyme activity was significantly decreased by 44% in PCC rats ($p = 0.03$) compared to PF rats (Figure 3 C).

Liver CL remodeling processes are affected by cancer cachexia

We previously reported important modifications in CL fatty acid composition in liver mitochondria from cachectic rats [7] suggesting a modulation in CL remodeling. We examined four enzymes implicated in this process: iPLA2 γ , MLCL AT-1, ALCAT1 and TAZ in livers of healthy (PF) and cachectic rats (PCC). iPLA2 γ enzyme activity and mRNA expression were not different from PCC and PF rats (mRNA: 0.64 \pm 0.25 vs 0.88 \pm 0.30 and activity: 767 \pm 160 vs 823 \pm 46 pmol.mg⁻¹.min⁻¹, respectively). In addition

MLCL AT-1 enzyme activity was significantly increased by 30% in PCC rat liver mitochondria compared to PF rats ($p = 0.01$) (Figure 3 D). ALCAT1 mRNA expression was similar in liver between PCC and PF rats (1.24 ± 0.28 vs 1.27 ± 0.19 , respectively). Finally, TAZ mRNA expression was significantly increased (50%) in PCC rats compared to PF rats ($p = 0.02$) (Figure 3 E).

TNF α treatment increases specifically hepatocyte CL content without changes in mitochondrial mass

Since TNF α was elevated 14-fold in plasma in rat model of peritoneal carcinosis induced cancer cachexia, the effect of exogenous TNF α addition to HepaRG cells on CL metabolism was examined. Incubation of HepaRG cells with TNF α resulted in a significant 15% ($p < 0.05$) increase in CL content compared to controls (Figure 4 A). In contrast, PE, PI, PC+PS and SM content did not differ between control cells and TNF α treated cells. In order to confirm that CL accumulation in response to TNF α was not due to an increase in mitochondrial mass, we quantified mitochondria area and number per cell area using transmission electron microscopy (Figure 4 B, C and D). Our result clearly demonstrated that TNF α has no effect on mitochondrial content (Control: $10.12\% \pm 0.33$, TNF α : $10.26\% \pm 0.30$ mitochondrial area % of cell area).

TNF α treatment alters HepaRG mitochondrial bioenergetics

Since CL plays a role in cellular energy metabolism and CL content was elevated in HepaRG cells treated with TNF α , we examined oxygen consumption in these cells. In intact HepaRG cells TNF α induced an overall increase in O₂ consumption (Figure 5). In fact, under routine conditions (cells using their own substrates in an energetic state with ATP production as a function of the energy needs of the cells) O₂ consumption was 33% higher in cells incubated with TNF α compared to control cells (figure 5 A). In the non-phosphorylating state, O₂ consumption (reflecting energy leak) in the presence of oligomycin, was significantly increased by 57% in cells treated with TNF α compared to controls. TNF α induced a significant 53% increase in maximal O₂ consumption (uncoupled state, electron transport chain maximal capacities ETS) compared to controls (figure 5A). When cells were permeabilized, we observed globally the same effect of TNF α on mitochondrial bioenergetics using pyruvate, malate and succinate as

substrates (Figure 5 B). O₂ consumption in non-phosphorylating (state 4) was significantly increased 33% in TNF α -treated cells compared to control cells (figure 5B). In the phosphorylating state (state 3), TNF α treated cells had a 17% significant increase in O₂ consumption compared to controls. Finally, uncoupled state related- O₂ consumption was increased 14% with TNF α compared to controls, however, this did not reach statistical significance (figure 5 B).

TNF α treatment increases PGPS gene expression in HepaRG cells

We examined the mechanism for the increase in CL in TNF α -treated cells. Incubation of HepaRG cells with TNF α did not affect mRNA expression of PGPP or CLS compared to controls (Figure 6 A and C). In contrast, PGPS mRNA expression was significantly increased 44% in cells incubated with TNF α compared to controls (Figure 6 B). Interestingly, incubation of HepaRG cells with TNF α did not affect TAZ, MLCL AT-1 or ALCAT1 mRNA expression (Figure 6 D, E and F). In addition, incubation of HepaRG cells with TNF α did not affect enzyme activities of CDS, PGPS and CLS compared to controls (Figure 7 A, B and C). In contrast, MLCL AT-1 activity was significantly increased 20% in cells treated with TNF α compared to controls (Figure 7 D).

TNF α treatment alters CL fatty acid molecular species in HepaRG cells

Next we asked if TNF α induced increase in MLCL AT-1 activity was associated to modification in CL molecular species. In fact, CL molecular species (18:1)₃-(18:2) and (18:2)₃-(16:1), have significantly altered content, respectively +15% and -10%, in TNF α treated hepatocytes compared to controls (Figure 8). Furthermore (16:0)-(18:1)₂-(18:2) and (18:1)₄ content was increased by 17% and 20% in HepaRG cells incubated with TNF α , without reaching statistical significance (p= 0.08) (Figure 8).

TNF α increases CL content by PGPS upregulation in HepaRG cells

Next we tested the direct connection between TNF α , CL content and PGPS expression. PGPS expression in siPGPS HepaRG cells was significantly reduced by 63 % in comparison of siALB cells (0,37 +/- 0,07

vs 1.00 +/- 0.11, relative expression/TBP respectively, N=4, p=0.028). Moreover, CL content was not affected by TNF α in siPGPS cells compared to controls (figure 9).

ACCEPTED MANUSCRIPT

DISCUSSION

The aim of the present study was to investigate the mechanisms responsible for liver mitochondrial CL accumulation and alteration of CL fatty acyl composition in a preclinical model of cancer cachexia. For this purpose, we examined gene and protein expression and activities of the main enzymes involved in CL biosynthesis and remodeling in liver mitochondria using a preclinical model of cancer cachexia. In addition, we investigated *in vitro* the effect of the proinflammatory cytokine TNF α , a hallmark of cancer cachexia, on CL content and the CL metabolic enzymes in HepaRG hepatocyte like cells.

We observed discordant regulation of CL biosynthetic and remodeling enzymes at both the activity and gene expression level in liver mitochondria of cachectic rats compared to controls. We found that gene expression of PGPS and TAZ were significantly increased and that enzyme activities of PGPS (statistical trend -30%) and MLCL AT-1 were increased and enzyme activity of CLS decreased in liver from cancer cachexia rats. PGPS catalyzes the committed step of CL biosynthesis [14]. The observed elevated mRNA expression and activity of PGPS in livers of PCC rats might increase precursor supply for CL *de novo* synthesis. A previous study showed increased liver CL pool size was associated with an increased expression and activity of PGPS during rat liver regeneration [31]. Moreover, the importance of PGPS in controlling CL level was previously demonstrated in Chinese hamster ovary (CHO) cells [32]. In that study, a temperature sensitive CHO cell line defective in PGPS exhibited reduced cellular levels of CL. CLS mRNA and protein expression were unaltered in liver of PCC rats compared to PF rats. Surprisingly, CLS enzyme activity was reduced approximately 50% in liver mitochondria of PCC rats compared to PF rats. The observed decrease in CLS activity could be a compensatory mechanism to counteract the increased CL formed in liver of PCC rats. We previously showed that CLS mRNA expression does not correlate with endogenous CLS enzyme activity [33]. In *Micrococcus lysodeikticus* the end-product of CL synthesis, CL, was shown to inhibit CLS at several concentrations [34]. In addition, in rat liver mitochondria exogenous addition of CL was shown to markedly inhibit CLS activity [35]. Since CL levels were elevated in liver mitochondria of cachectic rats this would explain why CLS enzyme activity was reduced. Thus, although CLS activity was decreased by a higher level of CL, the elevated

mRNA expression of PGPS could lead to an increase in precursor synthesis for increased CL *de novo* biosynthesis provoking CL accumulation in livers of cachectic rats. These data represent the first direct demonstration of dysregulation of CL biosynthesis in cancer cachexia.

We previously observed a lower n-6/n-3 polyunsaturated fatty acid ratio in CL in liver mitochondria prepared from cancer cachectic rats [7]. Liver CL is enriched with linoleic acid and this polyunsaturated fatty acid enrichment of CL can be achieved by a CL transacylase encoded by the *Taz* gene [36] or by transfer of linoleoyl-CoA to MLCL by MLCL AT-1 [37]. Gene expression of ALCAT1, an enzyme capable of acylating MLCL with polyunsaturated species of fatty acid to form polyunsaturated fatty acid enriched CL [15], was unaltered in liver of PCC rats compared to PF rats. In addition, the activity of iPLA2 γ , an enzyme known to deacylate CL [13], was unaltered in PCC rats compared to PF rats. In contrast, we observed a significant increase in both MLCL AT-1 enzyme activity and in TAZ mRNA expression. This increase in TAZ expression and MLCL AT-1 enzyme activity in liver of PCC rats was likely responsible for the altered fatty acid profile of CL observed in liver cachexia compared to control animals [7].

Since inflammation is a hallmark of cancer cachexia [20], we investigated the potential role of inflammatory cytokines in CL related-mitochondrial bioenergetics alterations in HepaRG hepatocytes. We previously identified TNF α as a major cytokine in our preclinical model of cancer cachexia [6]. In addition, an increased expression of TNF α has been observed in liver of cancer cachectic rats [38]. Therefore we examined *in vitro* the effects of TNF α treatment on HepaRG cell CL metabolism. Incubation with TNF α for 12 h increased mitochondrial CL content by 15% in HepaRG cells without affecting the level of other phospholipids. This increase in CL content was not related to an increase in mitochondrial mass in the cells treated with TNF α . We subsequently explored whether this increase in CL content in HepaRG cell mitochondria, mediated by TNF α , was associated with modification in mitochondrial bioenergetics. TNF α -treatment resulted in a significant increase in oxygen consumption in different energy states. The effect of TNF α on mitochondrial bioenergetics is subject to debate. Previous studies reported that TNF α treated cells exhibited inhibition of respiratory chain activity leading to enhanced superoxide production and apoptosis [39–42]. In contrast, other studies have demonstrated an increase in

mitochondrial oxygen consumption in TNF α treated cells [43–45]. This discrepancy highlights the fact that TNF α -mediated effects are very much dependent on cell type, cytokine concentration and treatment duration making comparison between studies difficult. However, our results are in agreement with recently published data by Drabarek and collaborators [44] in that our experimental protocol closely resembled their experimental conditions (hepatocyte cells, short term exposure and low TNF α concentration). Since mitochondrial biogenesis markers PGC-1 α and mitochondrial transcription factor A protein expression were unaffected by TNF α treatment (data not shown), the increase in oxygen consumption by 30-40% (depending of cell configuration) in the non-phosphorylating state was clearly an indication for an increase in energy wasting. Furthermore, we previously demonstrated that in cancer cachexia, CL content of rat liver biopsies are increased and positively correlated to energy wasting in mitochondria [7]. Moreover, we successfully reproduced *in vitro* this effect by mitochondrial membrane CL enrichment demonstrating a direct link between CL content and oxidative phosphorylation efficiency [8]. Taken together, all of these results indicate that TNF α may induce increase energy wasting in hepatocytes *in vivo* by increasing CL content.

Since *in vitro* treatment of HepaRG cells with TNF α increased CL content and energy wasting similar to what we previously observed in cachectic rat liver biopsies [7], we postulated that TNF α signaling regulated specifically PGPS gene expression in cancer cachexia and resulting in the increase in CL. Previously we showed that incubation of H9c2 cells with TNF α induced an increase in PGPS [46]. Thus, we investigated if TNF α regulated gene expression of PGPS and other CL metabolism related enzymes in HepaRG cells. A 12 h treatment of HepaRG cells with TNF α resulted in an increase in PGPS gene expression and an increase in MLCL AT-1 activity. These data are in agreement with previous published data demonstrating a TNF α induced-PGPS overexpression in cardiomyocyte cell line [46]. Moreover we had previously shown that MLCL AT-1 activity is regulated in concert with the level of CL and CL biosynthesis in rat heart [47]. The observed increase in MLCL AT-1 activity after treatment of HepaRG cells with TNF α is likely required to support elevated CL remodeling with increased CL synthesis. In support of this were the observed alterations in CL fatty acid molecular species composition.

Finally, the absence of modification in CL content in siRNA PGPS-transfected HepaRG cells exposed to TNF α highlighted that action of TNF α on CL content is mediated by PGPS.

In conclusion, this is the first study that demonstrates alteration in liver CL metabolism related enzymes in cancer cachexia. In addition, our data clearly demonstrate that TNF α treatment increases CL content in hepatocytes. These data strongly suggest that in cancer cachexia, TNF α is one of the factors responsible for inducing the increase in energy wasting in liver mitochondria by increasing CL content through upregulation of PGPS expression.

Acknowledgements

This paper is dedicated to the memory of William A. Taylor who passed away prematurely during this study. This work was funded by “Ligue contre le Cancer” (16, 18, 37, 72 and 85 committees), Région Centre (LIPIDS project of ARD2020-Biomedicaments), “Cancéropole Grand Ouest”, “Groupe Lipides Nutrition” and “Association CANCEEN”. Laure Peyta received a fellowship from “Ministère de l’Enseignement Supérieur et de la Recherche ». We thank Fred Xu for PGPS enzyme activity assays. This work was supported by grants from the CIHR and Heart and Stroke Foundation of Canada (G.M.H.). G.M.H. is a Canada Research Chair in Molecular Cardiolipin Metabolism.

References

- [1] K. Fearon, F. Strasser, S.D. Anker, I. Bosaeus, E. Bruera, R.L. Fainsinger, et al., Definition and classification of cancer cachexia: an international consensus, *Lancet Oncol.* 12 (2011) 489–495. doi:10.1016/S1470-2045(10)70218-7.
- [2] W.D. Dewys, C. Begg, P.T. Lavin, P.R. Band, J.M. Bennett, J.R. Bertino, et al., Prognostic effect of weight loss prior to chemotherapy in cancer patients. Eastern Cooperative Oncology Group, *Am J Med.* 69 (1980) 491–497.
- [3] A. Laviano, M.M. Meguid, A. Inui, M. Muscaritoli, F. Rossi-Fanelli, Therapy insight: Cancer anorexia-cachexia syndrome--when all you can eat is yourself, *Nat Clin Pr. Oncol.* 2 (2005) 158–165. doi:10.1038/ncponc0112.
- [4] M. Pressoir, S. Desné, D. Berchery, G. Rossignol, B. Poiree, M. Meslier, et al., Prevalence, risk factors and clinical implications of malnutrition in French Comprehensive Cancer Centres., *Br. J. Cancer.* 102 (2010) 966–971. doi:10.1038/sj.bjc.6605578.
- [5] C.M. Prado, S. Antoun, M.B. Sawyer, V.E. Baracos, Two faces of drug therapy in cancer: drug-related lean tissue loss and its adverse consequences to survival and toxicity., *Curr. Opin. Clin. Nutr. Metab. Care.* 14 (2011) 250–4. doi:10.1097/MCO.0b013e3283455d45.
- [6] J.-F. Dumas, C. Goupille, M. Pinault, L. Fandeur, P. Bougnoux, S. Servais, et al., n-3 PUFA-enriched diet delays the occurrence of cancer cachexia in rat with peritoneal carcinosis, *Nutr Cancer.* 62 (2010) 343–350. doi:10.1080/01635580903407080.
- [7] J.-F. Dumas, C. Goupille, C.M. Julianne, M. Pinault, S. Chevalier, P. Bougnoux, et al., Efficiency of oxidative phosphorylation in liver mitochondria is decreased in a rat model of peritoneal carcinosis, *J Hepatol.* 54 (2011) 320–327. doi:10.1016/j.jhep.2010.08.012.
- [8] C.M. Julianne, M. Tardieu, S. Chevalier, M. Pinault, P. Bougnoux, F. Labarthe, et al., Cardiolipin content is involved in liver mitochondrial energy wasting associated with cancer-induced cachexia without the involvement of adenine nucleotide translocase., *Biochim. Biophys. Acta.* 1842 (2014) 726–33. doi:10.1016/j.bbdis.2014.02.003.
- [9] J. Lecoq, C. Ballou, On the structure of cardiolipin., *Biochemistry.* 3 (1964) 976–80.
- [10] G. Paradies, V. Paradies, V. De Benedictis, F.M. Ruggiero, G. Petrosillo, Functional role of cardiolipin in mitochondrial bioenergetics., *Biochim. Biophys. Acta.* 1837 (2014) 408–17. doi:10.1016/j.bbabi.2013.10.006.
- [11] J. Zhang, Z. Guan, A.N. Murphy, S.E. Wiley, G.A. Perkins, C. a Worby, et al., Mitochondrial phosphatase PTPMT1 is essential for cardiolipin biosynthesis., *Cell Metab.* 13 (2011) 690–700. doi:10.1016/j.cmet.2011.04.007.
- [12] B. Lu, F.Y. Xu, Y.J. Jiang, P.C. Choy, G.M. Hatch, C. Grunfeld, et al., Cloning and characterization of a cDNA encoding human cardiolipin synthase (hCLS1)., *J. Lipid Res.* 47 (2006) 1140–5. doi:10.1194/jlr.C600004-JLR200.

- [13] Y.-H. Hsu, D.S. Dumlao, J. Cao, E.A. Dennis, Assessing phospholipase A2 activity toward cardiolipin by mass spectrometry., *PLoS One*. 8 (2013) e59267. doi:10.1371/journal.pone.0059267.
- [14] E.M. Mejia, L.K. Cole, G.M. Hatch, Cardiolipin metabolism and the role it plays in heart failure and mitochondrial supercomplex formation., *Cardiovasc. Hematol. Disord. Drug Targets*. 14 (2014) 98–106.
- [15] J. Cao, Y. Liu, J. Lockwood, P. Burn, Y. Shi, A novel cardiolipin-remodeling pathway revealed by a gene encoding an endoplasmic reticulum-associated acyl-CoA:lysocardiolipin acyltransferase (ALCAT1) in mouse., *J. Biol. Chem*. 279 (2004) 31727–34. doi:10.1074/jbc.M402930200.
- [16] M. Ren, C.K.L. Phoon, M. Schlame, Metabolism and function of mitochondrial cardiolipin., *Prog. Lipid Res*. 55 (2014) 1–16. doi:10.1016/j.plipres.2014.04.001.
- [17] M.G. Baile, Y.-W. Lu, S.M. Claypool, The topology and regulation of cardiolipin biosynthesis and remodeling in yeast., *Chem. Phys. Lipids*. 179 (2014) 25–31. doi:10.1016/j.chemphyslip.2013.10.008.
- [18] Y.J. Jiang, B. Lu, F.Y. Xu, J. Gartshore, W.A. Taylor, A.J. Halayko, et al., Stimulation of cardiac cardiolipin biosynthesis by PPARalpha activation, *J Lipid Res*. 45 (2004) 244–252. doi:10.1194/jlr.M300314-JLR200.
- [19] L. Lai, M. Wang, O.J. Martin, T.C. Leone, R.B. Vega, X. Han, et al., A role for peroxisome proliferator-activated receptor γ coactivator 1 (PGC-1) in the regulation of cardiac mitochondrial phospholipid biosynthesis., *J. Biol. Chem*. 289 (2014) 2250–9. doi:10.1074/jbc.M113.523654.
- [20] J.K. Onesti, D.C. Guttridge, Inflammation based regulation of cancer cachexia., *Biomed Res. Int*. 2014 (2014) 168407. doi:10.1155/2014/168407.
- [21] P. Gripon, S. Rumin, S. Urban, J. Le Seyec, D. Glaire, I. Cannie, et al., Infection of a human hepatoma cell line by hepatitis B virus., *Proc. Natl. Acad. Sci. U. S. A*. 99 (2002) 15655–60. doi:10.1073/pnas.232137699.
- [22] G.M. Hatch, G. McClarty, Regulation of cardiolipin biosynthesis in H9c2 cardiac myoblasts by cytidine 5'-triphosphate., *J. Biol. Chem*. 271 (1996) 25810–6.
- [23] V. Laurent, A. Fraix, T. Montier, S. Cammas-Marion, C. Ribault, T. Benvegna, et al., Highly efficient gene transfer into hepatocyte-like HepaRG cells: New means for drug metabolism and toxicity studies, *Biotechnol. J*. 5 (2010) 314–320. doi:10.1002/biot.200900255.
- [24] E.G. Bligh, W.J. Dyer, A rapid method of total lipid extraction and purification., *Can. J. Biochem. Physiol*. 37 (1959) 911–7.
- [25] M. Arvier, L. Lagoutte, G. Johnson, J.F. Dumas, B. Sion, G. Grizard, et al., Adenine nucleotide translocator promotes oxidative phosphorylation and mild uncoupling in mitochondria after dexamethasone treatment, *Am J Physiol Endocrinol Metab*. 293 (2007) E1320–4.
- [26] J. Folch, M. Lees, G.H. Sloane Stanley, A simple method for the isolation and purification of total lipides from animal tissues., *J. Biol. Chem*. 226 (1957) 497–509.

- [27] G. Vial, M.-A. Chauvin, N. Bendridi, A. Durand, E. Meugnier, A.-M. Madec, et al., Imeglimin Normalizes Glucose Tolerance and Insulin Sensitivity and Improves Mitochondrial Function in Liver of a High-Fat High-Sucrose Diet Mice Model., *Diabetes*. (2014). doi:10.2337/db14-1220.
- [28] W.A. Taylor, G.M. Hatch, Purification and characterization of monolysocardiolipin acyltransferase from pig liver mitochondria., *J. Biol. Chem.* 278 (2003) 12716–21. doi:10.1074/jbc.M210329200.
- [29] M. Schlame, K.Y. Hostetler, Mammalian cardiolipin biosynthesis., *Methods Enzymol.* 209 (1992) 330–7.
- [30] W. a Taylor, G.M. Hatch, Identification of the human mitochondrial linoleoyl-coenzyme A monolysocardiolipin acyltransferase (MLCL AT-1)., *J. Biol. Chem.* 284 (2009) 30360–71. doi:10.1074/jbc.M109.048322.
- [31] J. Webster, J.Y. Jiang, B. Lu, F.Y. Xu, W.A. Taylor, M. Mymin, et al., On the mechanism of the increase in cardiolipin biosynthesis and resynthesis in hepatocytes during rat liver regeneration., *Biochem. J.* 386 (2005) 137–43. doi:10.1042/BJ20040655.
- [32] T. Ohtsuka, M. Nishijima, Y. Akamatsu, A somatic cell mutant defective in phosphatidylglycerophosphate synthase, with impaired phosphatidylglycerol and cardiolipin biosynthesis., *J. Biol. Chem.* 268 (1993) 22908–13.
- [33] B. Lu, F.Y. Xu, W. a Taylor, K.R. Feingold, G.M. Hatch, Cardiolipin synthase-1 mRNA expression does not correlate with endogenous cardiolipin synthase enzyme activity in vitro and in vivo in mammalian lipopolysaccharide models of inflammation., *Inflammation*. 34 (2011) 247–54. doi:10.1007/s10753-010-9230-3.
- [34] A.J. De Siervo, Inhibition of cardiolipin synthesis by end-products and other complex lipids in membrane preparations of *Micrococcus lysodeikticus*., *Can. J. Biochem.* 53 (1975) 1031–4.
- [35] W.C. McMurray, E.C. Jarvis, Partial purification of diphosphatidylglycerol synthetase from liver mitochondrial membranes., *Can. J. Biochem.* 58 (1980) 771–6.
- [36] S. Bione, P. D'Adamo, E. Maestrini, A.K. Gedeon, P.A. Bolhuis, D. Toniolo, A novel X-linked gene, G4.5. is responsible for Barth syndrome., *Nat. Genet.* 12 (1996) 385–9. doi:10.1038/ng0496-385.
- [37] B.J. Ma, W.A. Taylor, V.W. Dolinsky, G.M. Hatch, Acylation of monolysocardiolipin in rat heart., *J. Lipid Res.* 40 (1999) 1837–45.
- [38] M.G. Catalano, N. Fortunati, K. Arena, P. Costelli, M. Aragno, O. Danni, et al., Selective up-regulation of tumor necrosis factor receptor I in tumor-bearing rats with cancer-related cachexia., *Int. J. Oncol.* 23 (2003) 429–36.
- [39] S. Djafarzadeh, M. Vuda, J. Takala, S.M. Jakob, Effect of remifentanyl on mitochondrial oxygen consumption of cultured human hepatocytes., *PLoS One*. 7 (2012) e45195. doi:10.1371/journal.pone.0045195.
- [40] R. Zell, P. Geck, K. Werdan, P. Boekstegers, TNF-alpha and IL-1 alpha inhibit both pyruvate dehydrogenase activity and mitochondrial function in cardiomyocytes: evidence for primary impairment of mitochondrial function., *Mol. Cell. Biochem.* 177 (1997) 61–7.

- [41] J. Stadler, B.G. Bentz, B.G. Harbrecht, M. Di Silvio, R.D. Curran, T.R. Billiar, et al., Tumor necrosis factor alpha inhibits hepatocyte mitochondrial respiration., *Ann. Surg.* 216 (1992) 539–46.
- [42] J.R. Lancaster Jr., S.M. Laster, L.R. Gooding, J.R. Lancaster, Inhibition of target cell mitochondrial electron transfer by tumor necrosis factor, *FEBS Lett.* 248 (1989) 169–174.
- [43] L. Kastl, S.W. Sauer, T. Ruppert, T. Beissbarth, M.S. Becker, D. Süss, et al., TNF- α mediates mitochondrial uncoupling and enhances ROS-dependent cell migration via NF- κ B activation in liver cells., *FEBS Lett.* 588 (2014) 175–83. doi:10.1016/j.febslet.2013.11.033.
- [44] B. Drabarek, D. Dymkowska, J. Szczepanowska, K. Zabłocki, TNF α affects energy metabolism and stimulates biogenesis of mitochondria in EA.hy926 endothelial cells., *Int. J. Biochem. Cell Biol.* 44 (2012) 1390–7. doi:10.1016/j.biocel.2012.05.022.
- [45] S. Busquets, X. Aranda, M. Ribas-Carbó, J. Azcon-Bieto, F.J. López-Soriano, J.M. Argilés, et al., Tumour necrosis factor-alpha uncouples respiration in isolated rat mitochondria, *Cytokine*. 22 (2003) 1–4.
- [46] F.Y. Xu, S.L. Kelly, G.M. Hatch, N-Acetylsphingosine stimulates phosphatidylglycerolphosphate synthase activity in H9c2 cardiac cells., *Biochem. J.* 337 (1999) 483–90.
- [47] W. a Taylor, F.Y. Xu, B.J. Ma, T.C. Mutter, V.W. Dolinsky, G.M. Hatch, Expression of monolysocardiolipin acyltransferase activity is regulated in concert with the level of cardiolipin and cardiolipin biosynthesis in the mammalian heart., *BMC Biochem.* 3 (2002) 9. doi:10.1186/1471-2091-3-9.

Figure legends

Figure 1: Liver mitochondrial mass is unchanged during cancer cachexia. (A) mitochondrial area quantification with (B) and (C) example of electron microscopy image from liver of PF and PCC rat. Values represent the mean \pm SEM. Pair-fed rats (PF, white bar) and peritoneal carcinosis induced cachexia rats (PCC, black bar) with N = 3 per group.

Figure 2: Liver PGPS gene expression is upregulated in cancer cachexia. (A) CDS1 relative expression normalized to 18S mRNA, (B) activity and (C) PGPS relative expression normalized to 18S mRNA (D) PGPS activity. Values represent the mean \pm SEM. Pair-fed rats (PF, white bar) and peritoneal carcinosis induced cachexia rats (PCC, black bar) with N = 7 per group. * $p < 0.05$ compared to PF.

Figure 3: Liver CLS activity is decreased whereas CL remodeling enzymes are upregulated in cachectic rats. (A) CLS relative expression normalized to 18S mRNA, (B) CLS protein expression normalized by Hsc70 protein expression, (C) CLS activity, (D) MLCL AT-1 liver activity and (E) TAZ relative expression normalized to 18S mRNA. Values represent the mean \pm SEM. Pair-fed rats (PF, white bar) and peritoneal carcinosis induced cachexia rats (PCC, black bar) with N = 7 per group. * $p < 0.05$ compared to PF.

Figure 4: TNF α treatment of HepaRG cells results in increased CL content without modification of mitochondrial mass. Cells were treated for 12 h with 20 ng/ml of TNF α . (A) Mitochondrial phospholipid content with Cardiolipin (CL), phosphatidylethanolamine (PE), phosphatidylinositol (PI), phosphatidylcholine and phosphatidylserine (PC+PS), and sphingomyelin [SM]. Values represent the mean \pm SEM (N = 6 per group). White bars: control treatment; black bars: TNF α treatment. * $p < 0.05$, compared to control treatment. (B) Mitochondrial area in % of HepaRG area. (C) and (D) example of electronic microscopic images of HepaRG cells in control condition and TNF α treatment, respectively.

Figure 5: TNF α treatment of HepaRG cells results in increased O₂ consumption. Cells were treated for 12 h with 20 ng/ml of TNF α and then high resolution respirometry performed on (A) intact cells or on (B)

permeabilized cells using pyruvate, malate and succinate as substrate. Values represent the mean oxygen (O_2) consumption (pmol / min / 10^6 cells) \pm SEM (N= 6 per group). White bars: control treatment; black bars: TNF α treatment. * $p < 0.05$, ** $p < 0.01$ compared to control treatment.

Figure 6: TNF α treatment results in increased PGPS gene expression in HepaRG cells. Gene expression of (A) PGPP, (B) PGPS, (C) CLS, (D) MLCL AT-1, (E) Tafazzin and (F) ALCAT1. Cells were treated for 12 h with 20 ng/ml of TNF α . Total RNA was isolated and mRNA expression of the above genes determined. Values are normalized by GAPDH expression. Values represent the mean \pm SEM (N = 9 per group). White bars: control treatment; black bars: TNF α treatment. **** $p < 0.0001$, compared to control treatment.

Figure 7: TNF α treatment of HepaRG cells increases MLCL AT-1 activity. HepaRG cells were treated for 12 h with 20 ng/ml of TNF α and activity of (A) CDS1, (B) PGPS, (C) CLS and (D) MLCL AT-1 determined. Values represent the mean \pm SEM (N = 5 per group). White bars: control treatment; black bars: TNF α treatment. * $p < 0.05$ compared to control cells.

Figure 8: TNF α treatment of HepaRG cells affects fatty acid molecular species composition. HepaRG cells were treated for 12 h with 20 ng/ml of TNF α and CL fatty acid molecular species were analyzed (in % of total CL molecular species). Values represent the mean \pm SEM (N = 6 per group). White bars: control treatment; black bars: TNF α treatment. * $p < 0.05$, ** $p < 0.01$ compared to control treatment.

Figure 9: TNF α treatment does not affect CL content in HepaRG siPGPS cells. HepaRG cells (siPGPS) were treated for 12 h with 20 ng/ml of TNF α . Cardiolipin content (CL) in siPGPS HepaRG cells +/- TNF α . Values represent the mean \pm SEM (gene expression: N = 4 per group; cardiolipin content: N=4 per group). White bars: control treatment; black bars: TNF α treatment.

Figures

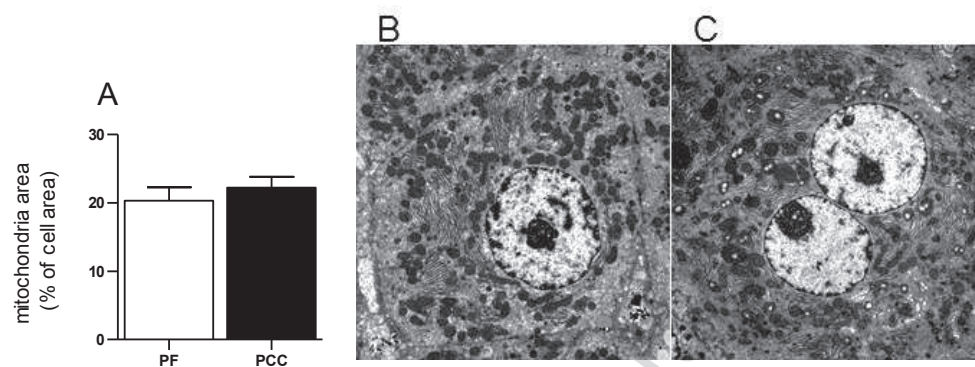
Figure 1: Liver mitochondrial mass is unchanged during cancer cachexia

Figure 2: Liver PGPS gene expression is upregulated in cancer cachexia.

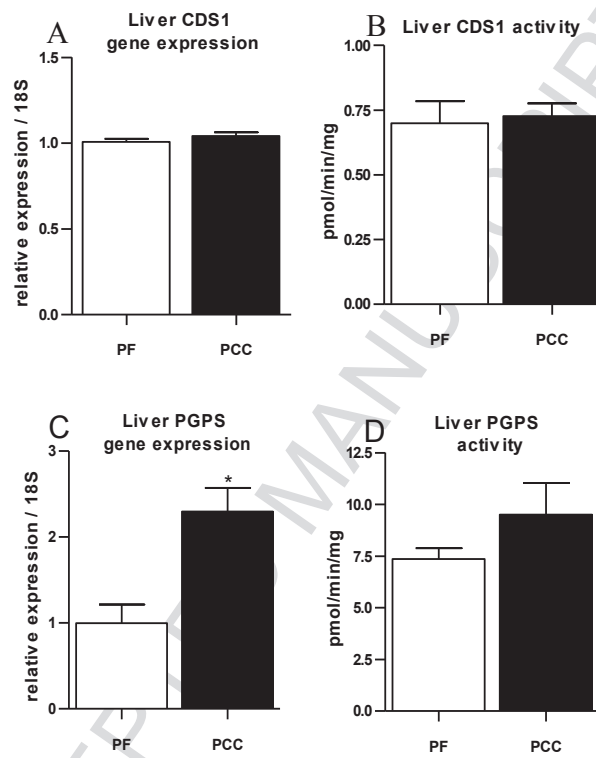


Figure 3: Liver CLS activity is decreased whereas CL remodeling enzymes are upregulated in cachectic rats.

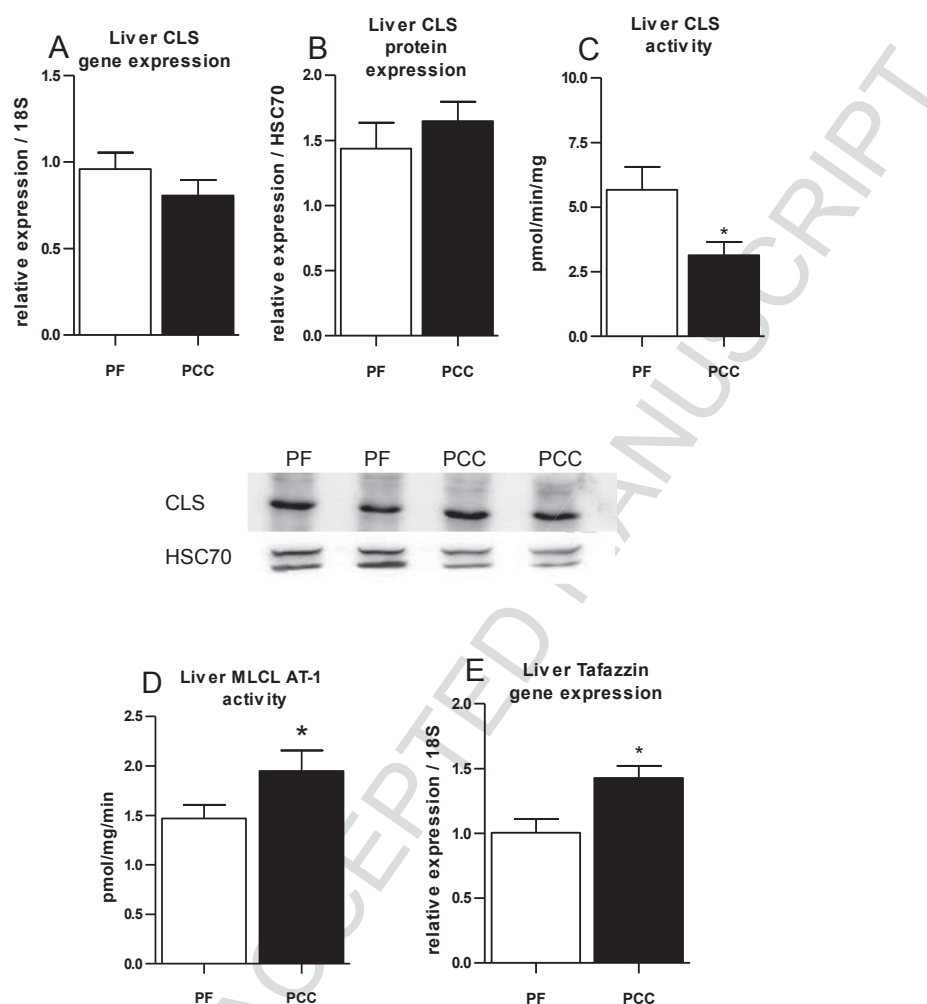


Figure 4: TNF α treatment of HepaRG cells results in increased CL content without modification of mitochondrial mass.

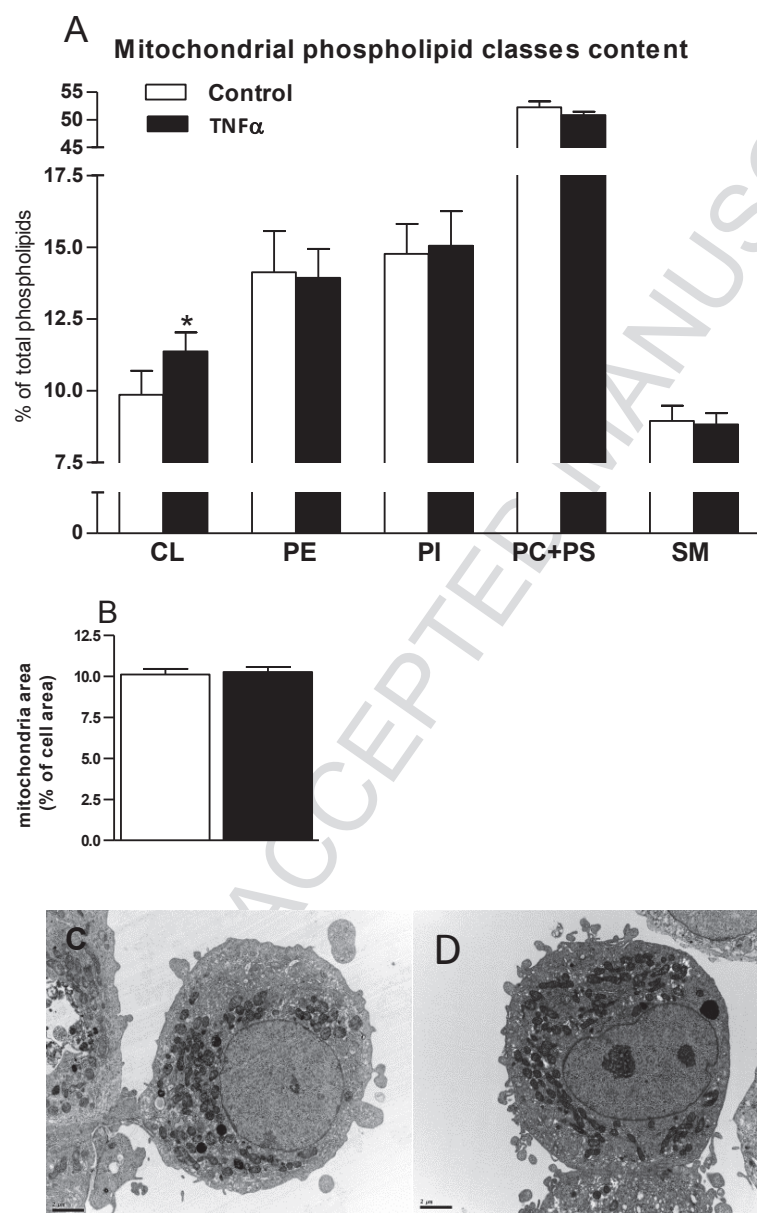


Figure 5: TNF α treatment of HepaRG cells results in increased O₂ consumption.

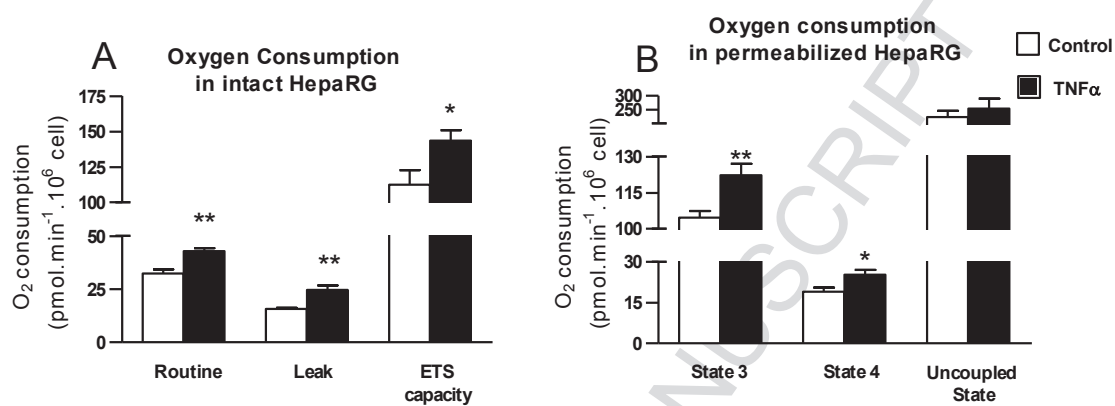


Figure 6: TNF α treatment results in increased PGPS gene expression in HepaRG cells.

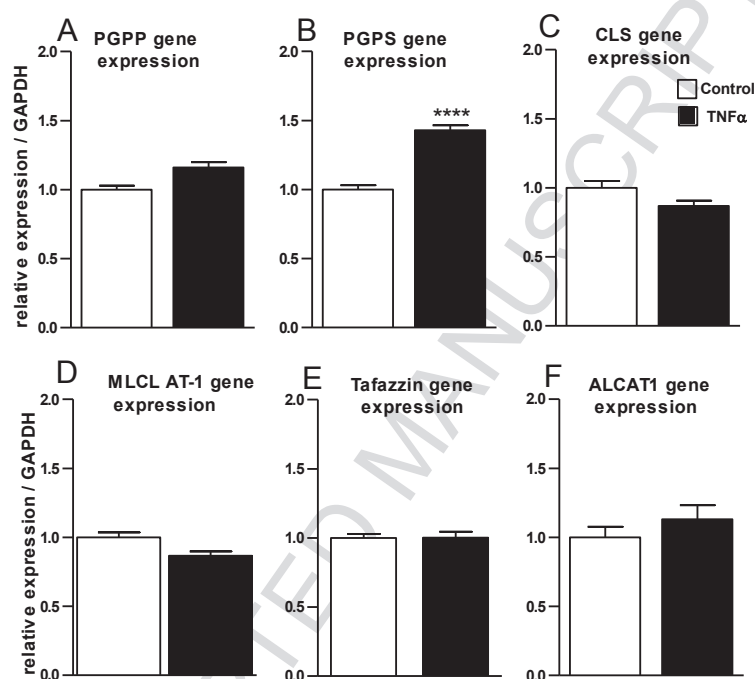
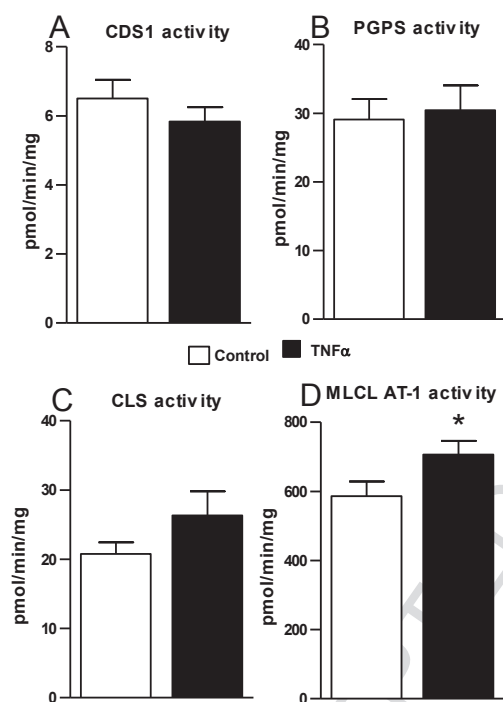


Figure 7: TNF α treatment of HepaRG cells increases MLCL AT-1 activity.



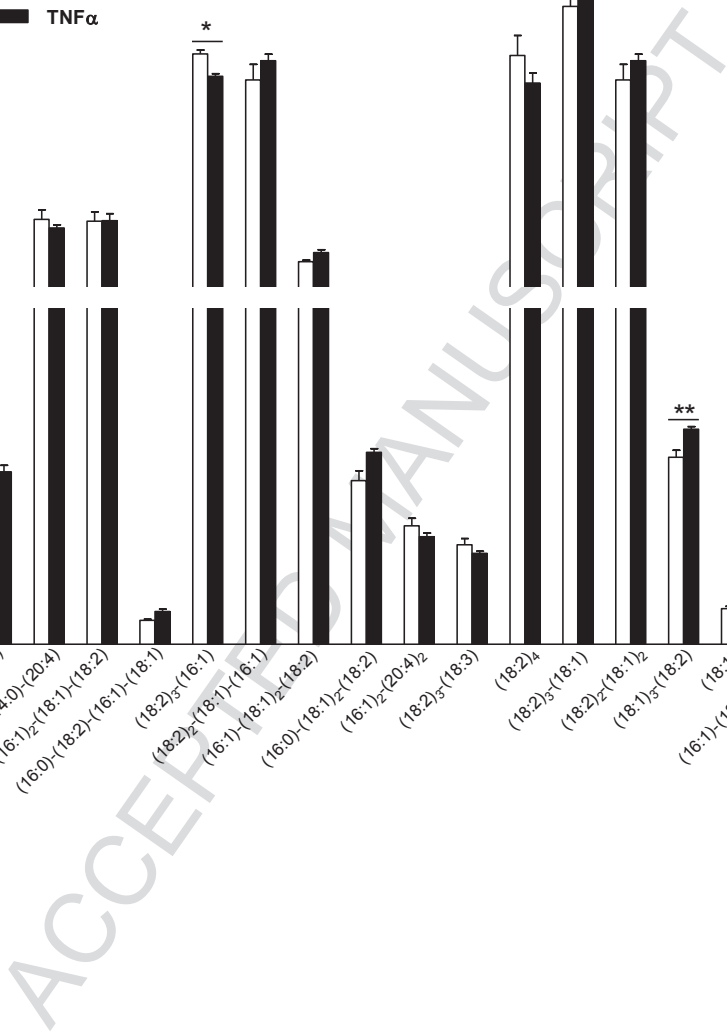
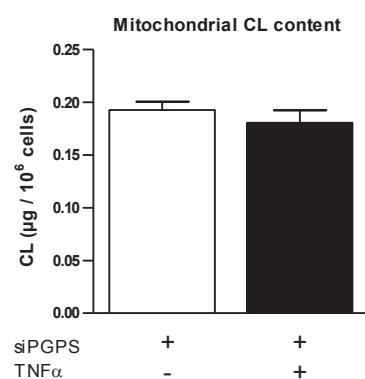


Figure 9: TNF α treatment does not affect CL content in HepaRG siPGPS cells



Conflict of interest

All the authors of the article « Regulation of hepatic cardiolipin metabolism by TNF α : implication in cancer cachexia” submitted to BBA- Molecular and Cell Biology of lipids, declare no conflict of interest.

Laure Peyta, Kathleen Jarnouen, Michelle Pinault, Cedric Coulouarn, Cyrille Guimaraes, Caroline Goupille, Jean-Paul Pais de Barros, Stephan Chevalier, Jean-François Dumas, François Maillot, Grant M. Hatch, Pascal Loyer and Stephane Servais have nothing to disclose.